ELSEVIER

Journal of Molecular Graphics and Modelling 21 (2002) 111–118

Journal of Molecular Graphics and Modelling

www.elsevier.com/locate/JMGM

Ligand-receptor interaction at the neural nicotinic acetylcholine binding site: a theoretical model

A. Morreale [a], F. Maseras [b], I. Iriepa [a], E. Gálvez [a,*]

[a] *Departamento de Química Orgánica, Facultad de Farmacia, Universidad de Alcalá, Ctra. Madrid-Barcelona Km. 33,600. 28871, Alcalá de Henares, Madrid, Spain*

[b] *Unitat de Química-Física, Edifici C.n., Universitat Autònoma de Barcelona, 08193 Bellaterra, Barcelona, Spain*

Received 28 October 2001; received in revised form 29 April 2002; accepted 29 April 2002

Abstract

Recent mutagenesis experiments have identified some of the functional amino acids that are essential in the interaction of nicotinic agents with the binding site of the neural nicotinic acetylcholine receptor (nAChR). Although this receptor is one of the best studied and characterized the lack of detailed experimental information regarding its quaternary structure has turned it into a challenge for computational chemistry. We have previously reported [J. Comput. Aided Mol. Design 13 (1999) 57–68] a computational protocol based on molecular mechanics and molecular dynamics (MD) where SER82, ASP83, TRP86, ASP89, TYR93, TYR190, TYR198 and ARG209 were placed around selected agonists and antagonists aided by stereoelectronic criteria. Explicit water molecules were used with the double goal of simulating aqueous environment and keeping the system from falling apart. The protocol was stable enough to allow the ligands to evolve to their thermodynamically most probable structure while maintaining the key interactions. In this communication we use the average model for the agonists (one average structure for each agonist) to calculate quantum mechanically the interactions of the binding site with one neurotransmitter acetylcholine (ACh, **1**), as well as with two of the most potent agonists described so far [nicotine (**2**) and epibatidine (**3**)] and the modeled binding site. A wide variety of methods as well as basis sets were used in order to rationalise the best way to treat the problem. In this limited set of compounds, a good correlation between total interaction energies and biological affinity is observed.

Keywords: nAChR; Acetylcholine; Epibatidine; Nicotine; Density functional

1. Introduction

There is an increasing interest in the quantitative characterization of ligand–protein interactions, an issue that can aid in the design of new drug candidates for the treatment of a wide variety of functional disorders. These disorders are associated with problems in the normal behaviour of some entities called receptors [1,2]. The recent advances in genomic as well as in the determination of solid structures for these systems have allowed three-dimensional (3D) structures be readily available for computer aided molecular design (CAMD) projects [3,4]. But there are still many receptors that because of the lack of this information or because the available data do not have an appropriate resolution, represent a challenge in the field as it is the case of $\alpha 4\beta 2$ neural nicotinic acetylcholine receptor (nAChR) [5,6].

nAChR is the best known and characterized member of a superfamily of receptors known as ligand-gatted ion channels receptors (LGIRs) and it is commonly used as the prototype for comparative studies [7–12]. All of these receptors are allosteric proteins with a hetero (or homo) pentameric arrangement of their subunits and with an overall arrangement as a five petal rose. Each subunit is in itself composed of a large extracellular N-terminal domain (where binding sites are located), four membrane-spanning segments and a short C-terminal domain. Once the neurotransmitter ACh (**1**, Fig. 1) has been released from the presynaptic neurone, it diffuses across the synaptic cleft interacting with nAChR located in the postsynaptic neurone surface. Then, some conformational changes take place and are transmitted along the polypeptide chain, reaching and opening the associated ion-channel, which finally allow the signal to be transmitted.

Although no accurate 3D structure for this receptor exists, so many families of compounds recognized by the receptor are known [13,14] and 3D-QSAR techniques are widely used in order to understand the main features of the binding [15–19]. Some other studies have been reported where acetylcholinesterase enzyme structure was used as starting point [20], but due to the low similarity between both sequences, the results are far from being conclusive.

* Corresponding author.

1093-3263/02/$ – see front matter
PII: S1093-3263(02)00127-4

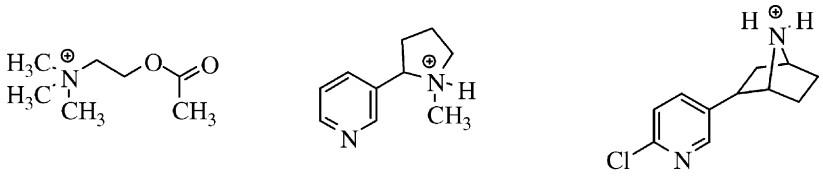

ACh (**1**) nicotine (**2**) epibatidine (**3**)

Fig. 1. Chemical diagrams for acetylcholine (**1**, ACh), nicotine (**2**), and epibatidine (**3**).

Alternatively, sequences alignment algorithms have also been employed to obtain a working image of the receptor [21,22]. In addition, other studies have reported quantitative data for these interactions, based mainly on hypothetical situations [23–27]. A recent review by Morreale et al. contains the more important contributions to this field till year 2000 [28]. Brejc et al. have recently reported the crystallographic structure of an ACh (**1**) binding protein, although it is a homopentameric (α) structure, it will be undoubtedly of great importance in future design projects [29].

In this contribution we use our previously obtained minireceptor for nAChR [26], so called because the amino acids building up the receptor cavity that surrounds the ligands were not linked. This was accomplished by means of molecular mechanics and molecular dynamic techniques obtaining some structural difference between agonists/antagonists binding site models. The main interactions occurring between three well known agonists [ACh (**1**), nicotine (**2**, Fig. 1) and epibatidine (**3**, Fig. 1)] and the hypothetical binding site just described are classified in groups and calculated through ab initio molecular orbital methods using B3LYP hybrid density functional model and 6–31+g basis set as wavefunction. The effect of the same groups in different ligands are compared, together with the total interaction energy (the energy gained upon binding) for each ligand-binding site complex. A good agreement is found between the total interaction energy and affinity data reported as pK_i values.[1] Moreover, due to the protocol employed, further comparisons between interaction groups gave a more detailed view of the main groups that contribute more to the total stabilization, a cornerstone information to aid in the design of new compounds with better pharmacological profiles.

2. Methodology

The three initial minireceptors were taken directly from the molecular dynamics (MD) results, each one obtained from a single MD run. Relevant details related with the minireceptor building and the computational protocol employed can be found in the original paper [26]. All the calculations were performed using Gaussian 98 program [30] running on IBM SP2 parallel computers (from CESCA/CEPBA).

2.1. Selection of basis set and computational method

A variety of basis sets and computational methods were tested to see which one provided the best ratio between quality and computational cost. The model chosen for these calculations was the interaction between the positive end in ACh (modeled as trimethylammonium cation) and one ASP residue (modeled as formate anion).

In order to test the basis set, single point (SP) RHF calculations were carried out on geometries optimized at the semiempirical level AM1 for both the separate trimethylammonium and formate systems and the interacting system containing both fragments, obtaining an interaction energy as the difference between both values (E_{INT}). The SP calculations were carried out with seven different basis sets: 6–31g, 6–31g*, 6–31g**, 6–31+g, 6–31++g, 6–31+g* and 6–31++g**. As it can be seen, the starting point was always the double-zeta basis set 6–31g, and the effect of adding diffuse (+) and/or polarization (*) functions was analyzed in a variety of combinations. The importance of diffuse and polarization and diffuse functions on hydrogen atoms (++ and ** basis sets) was also analyzed separately in order to look for the best combination of them to use in the study of these interactions. The results are summarized in Table 1.

Taking as starting point the 6–31g results, it can be seen that the sole addition of polarization functions, either including (6–31g**) or not (6–31g*) the hydrogen atoms, does not produce substantial changes in the interactions

Table 1
Effect of different basis sets on the ACh–ASP interaction energy

Model	E_{INT} (kcal/mol)
RHF/6–31g//AM1	−97.75
RHF/6–31g*//AM1	−97.34
RHF/6–31g**//AM1	−98.07
RHF/6–31+g//AM1	**−92.10**
RHF/6–31++g//AM1	−92.12
RHF/6–31+g*//AM1	−90.46
RHF/6–31++g**//AM1	−90.91

Selected basis set is highlighted in bold.

[1] pK_i affinity values were taken from [14]: 8.52 for ACh (**1**), 8.70 for nicotine (**2**), and 10.35 for epibatidine (**3**).

energies (less than 1 kcal/mol). Larger energy differences (above 5 kcal/mol) are observed, however, upon the introduction of diffuse functions in the second period atoms C, N and O (6–31+g basis set). No additional changes are added by the use of such functions on hydrogen atoms (6–31++g). The joint use of both kinds of basis set extensions (polarization and diffuse) does not greatly affect the interactions energies (changes always below 2 kcal/mol) compared with those obtained with only diffuse functions. The summary of this basis set analysis is therefore, that the only significant changes are related to the introduction of diffuse functions on second period atoms, and that further basis set extensions provide only a sharp increase in computer effort with little quality added. Therefore, the basis set to be used in this article will be 6–31+g. This result is by no means surprising because of the presence of negatively charged anionic groups, which are known to require diffuse functions for a proper description.

2.2. Selection of the computational method

After selecting the basis set it is also necessary to select a theoretical method. An approach based on SP calculations similar to that described above was used to deal with this problem. In this case, the trimethylammonium/formate system was also used, but the geometries were optimized at the RHF/6–31+g computational level.

Different methods were used, including semiempirical (AM1), Hartree–Fock based without correlation (RHF) and with correlation (MP2, CCSD(T)) and density functional-based (SVWN, B3LYP, BP86, BLYP). The most accurate method, and the most computationally demanding, among all of these is CCSD(T), and it was consequently chosen as providing the reference value. Fig. 2 shows graphically how the different methods deviate from this value.

Table 2
Different methods tested for the ACh–ASP interaction

Method	E_{INT} (kcal/mol)
AM1//RHF/6–31+g	−110.29
RHF/6–31+g//RHF/6–31+g	−98.20
MP2/6–31+g//RHF/6–31+g	−99.82
SVWN/6–31+g//RHF/6–31+g	−109.04
B3LYP/6–31+g//RHF/6–31+g	**−99.37**
BP86/6–31+g//RHF/6–31+g	−99.10
BLYP/6–31+g//RHF/6–31+g	−97.55
CCSD(T)/6–31+g//RHF/6–31+g	**−100.54**

Reference method (CCSD(T)) and chosen method (B3LYP) are highlighted in bold.

Numerical values for interaction energies obtained with the different computational methods are contained in Table 2. It can be seen from Fig. 2 and Table 2 that the two methods deviating more from the CCSD(T) reference value are the semiempirical AM1 and the local density functional approach SVWN. These two, which are the less computationally demanding, must be therefore discarded. The rest of the methods provide acceptable values within 3 kcal/mol of the reference value. MP2 seems to be in fact the second best method to use (behind CCSD(T)). The results afforded by B3LYP hybrid density functional method lie nevertheless very close to MP2. We decided to choose this latter B3LYP method in light of the demanding computational resources required by MP2 and the size of the different systems we are dealing with in this study.

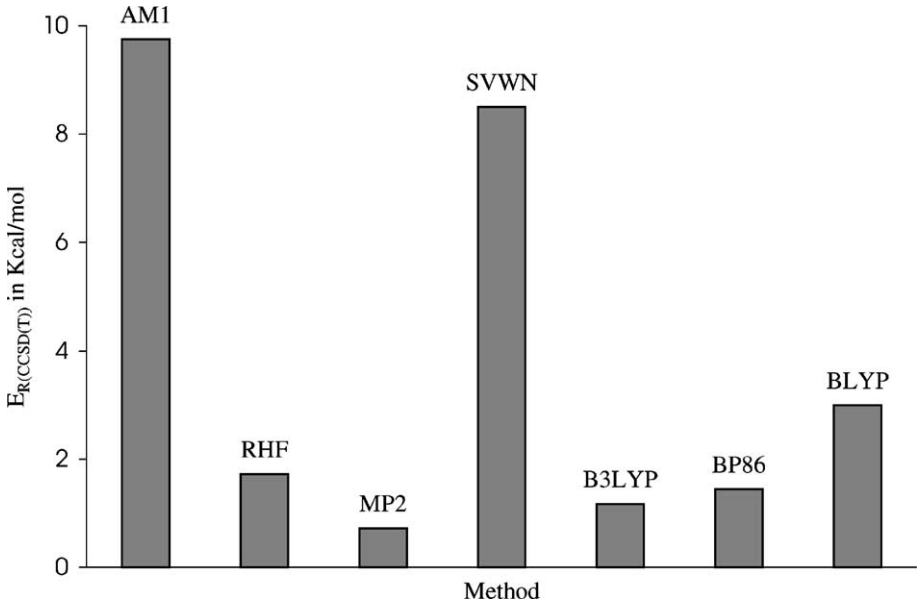

Fig. 2. Histogram showing deviation of the different theoretical methods used in this study for the ACh–ASP interaction energy. CCSD(T) was used as reference.

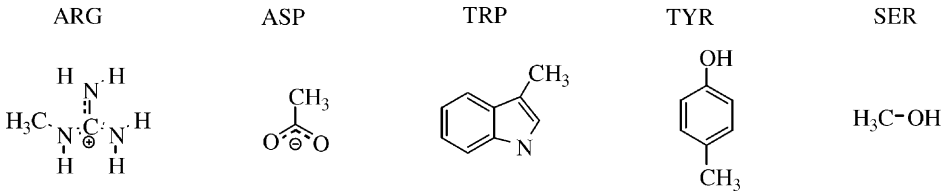

Fig. 3. Simple molecules used to represent the aminoacids side chain.

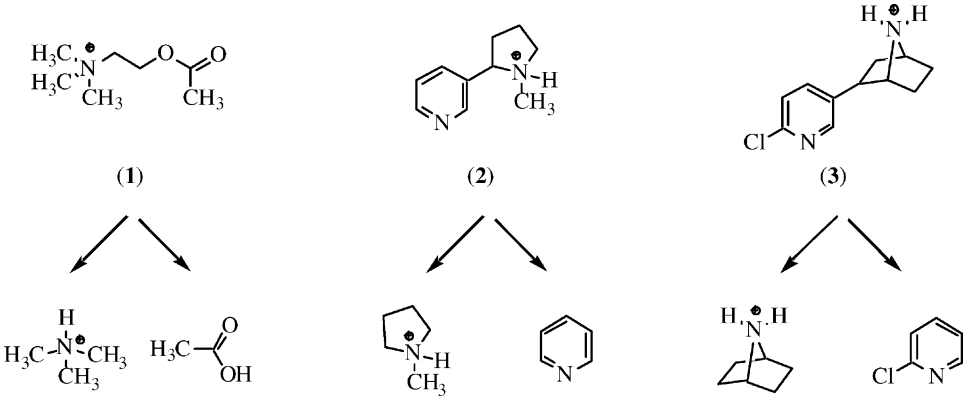

Fig. 4. Simple molecules used to represent positive and negative ends in the studied ligands.

3. Results and discussion

3.1. Computational strategy

Although the structures for the ligands ACh (**1**), nicotine (**2**), epibatidine (**3**); and for the aminoacids aspartic acid, tryptophan, tyrosine, arginine and serine are simple and well known, computing the full system including the ligand and the entire polypeptide sequence comprising the binding site using ab initio quantum mechanical methods is not feasible due to the high computer cost involved. To make this problem tractable only the pendant side chain of the aminoacids directly in contact with the ligand are considered in the computational model of the binding site. We chose the following simple molecules to represent the aminoacid side chains: methylguanidinium cation for arginine, formate anion for aspartic acid, 3-methyl-indole for trypophan, *p*-toluol for tyrosine and methanol for serine (Fig. 3).

A similar approach was followed for the ligands ACh (**1**), nicotine (**2**) and epibatidine (**3**). Each of them was divided into two interacting areas (Fig. 4): the positive end, which interacts with the negative (ASP83 and ASP89) and some neutral residues (SER82, TYR93 and TRP86) of the binding site; and the negative end, which interacts with the positive (ARG209) and the rest of the neutral residues (TYR190 and TYR198) of the binding site. The positive ends of ACh (**1**), nicotine (**2**) and epibatidine (**3**) were modeled as the trimethylammonium, *N*-methyl-pyrrolidine and azabicycle-[2.2.1]heptane cations, respectively. On the other hand, the negative ends were modeled as acetic acid, pyridine and 2-chloro-pyridine, respectively.

With these shortcuts being defined, we depict in Fig. 5 the computational strategy adopted here.

Even with these drastic simplifications, the calculation of the whole minireceptor would be extremely expensive. The idea is to calculate instead individual interactions between each fragment of the receptor and the ligand, and collect all of them to obtain the global stabilization energy. This pairwise analysis has the clear disadvantage of ignoring the interactions between the different fragments, and the effect the presence of one of them can have in the interaction of the ligand with the others. On the other hand, with this pairwise approach, more information can be retrieved than if the whole minireceptor was calculated, where only the

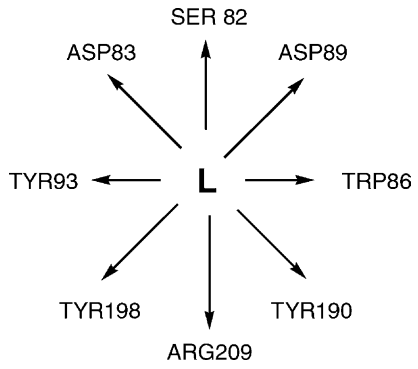

Fig. 5. A schematic representation of the pairwise approximation to calculate interactions between the binding site and the ligands.

information regarding the global stabilization is obtained. With the pairwise strategy the analysis of the results can be organized in three complementary ways: globally, by the type of interactions (ionic, π-cation, ...) and from the individual residue point of view.

The last aspect related to the computational strategy concerns the nature of the geometrical structures that must be used. One obvious choice would be the full optimization, but this would have the undesired side effect of completely ignoring the structure of the binding site, with the danger of going to unreasonable arrangements. Because of this, the first set of calculations will consist of SP calculations of the pairwise interactions described above with the ligand-fragment pairs frozen at the geometries generated by MD simulations for ACh (**1**), nicotine (**2**) and epibatidine (**3**) published in the literature [26]. Later on, the effect of geometry relaxation will be analyzed in detail in the case of one of the ligands.

3.2. Comparison between ACh (1), nicotine (2) and epibatidine (3)

SP calculations were performed in a pairwise fashion at B3LYP/6–31+g level of theory on the geometries taken directly from MD results. The first results worth commenting on are the total interaction energies The total energy of each complex was computed as the sum of the energies arising from the different interactions. The interaction happens to be much more stabilizing in the case of epibatidine (**3**, −182.51 kcal/mol), with a difference of ca. 30 kcal/mol with respect to the other two ligands. The interaction energies of ACh (**1**, −148.56 kcal/mol) and nicotine (**2**, −154.40 kcal/mol) are more similar, with the interaction of nicotine (**2**) being 5.84 kcal/mol more stabilizing than that of ACh (**1**). These results follow closely experimental data on biological affinity (see Footnote 1), thus providing support to the validity of the current analysis.

The analysis does not have to stop at the total interaction energies. A second level of analysis can be done separating the interaction energy by groups of fragments (Table 3). From a chemical point of view, the nine fragments can be divided in four groups depending on the type of interaction they have with the ligand. These groups are: ionic interactions with the positive end of the ligand (+) (ASP83, SER82, ASP89); π-cation interactions [31] with the positive end of the ligand (π-cation) (TYR93, TRP86); charge-transfer interactions with the negative end of the ligand (CTC) (TYR190, TYR198); and ionic interactions with the negative end of the ligand (−) (ARG209). The larger absolute values of interaction energy correspond logically to the ionic interaction with the positive end of the ligand, because these are the only interactions involving two charged fragments. The numbers would not be that large if the effects of solvent and counterions were considered, but the focus here is not in the absolute value, but in the comparison between the behavior of the three ligands, and the effect of solvent and counterion are likely to be of similar magnitude for the three of them.

Table 3
Binding interactions energies (kcal/mol) classified by type

Type	ACh	Nicotine	Epibatidine
(+)[a]	−138.40	−142.37	−159.12
π-Cation[b]	−4.79	−6.60	−9.86
CTC[c]	+3.51	+4.52	+0.26
(−)[d]	−8.88	−9.95	−13.79
Total	−148.56	−154.40	−182.51

SP approach at B3LYP/6–31+g level of theory.
[a] Interaction of ASP83, ASP89, and SER82 with the positive end of the ligands.
[b] Interaction of TYR93 and TRP89 with the positive end of the ligands.
[c] Interaction of TYR190 and TYR198 with the negative end of the ligands.
[d] Interaction of ARG203 with the negative end of the ligands.

The comparison shows that the difference in the (+) contribution, the interaction with the positive end of the ligand, is indeed the larger contribution, with a range of 20.72 kcal/mol, but it is obviously unable to explain the full difference between the ligands, which spans a range of 33.95 kcal/mol. The relative weight of the (+) term depends furthermore on the ligands under comparison. For instance, it accounts for 3.97 kcal/mol out of the 5.84 kcal/mol difference between ACh (1) and nicotine (68%); but only for 20.72 kcal/mol of the 33.95 kcal/mol difference between ACh (**1**) and epibatidine (61%). This (+) contribution defines in any case the overall trend, with nicotine (**2**) being slightly more active than ACh (**1**) and epibatidine (**3**) much more than the other two. The other terms have to be nevertheless also taken into account. Changes in each of them have similar weights. The (π-cation) contribution spans a range of 5.07 kcal/mol difference, while the respective values for the CTC and (−) contributions are 4.26 and 4.91 kcal/mol. The (π-cation) term plays a significantly more important role in defining the difference between ACh (**1**) and nicotine (**2**, 1.81 kcal/mol difference) than the (−) term (1.07 kcal/mol difference). Relative weights between them are inverted in the comparison between nicotine (**2**) and epibatidine (**3**), with the (−) block (3.84 kcal/mol) being more important than the (π-cation) one (3.26 kcal/mol). The case of the CTC contribution merits some additional comment. It is the only case where the interaction is not attractive, but slightly repulsive, and it is also the only case where the order of the values is not the same as that of the overall interaction. This interaction is more unfavorable for nicotine (**2**) than for ACh (**1**) by 1.01 kcal/mol, and in fact it nearly compensates the difference in the (−) term between this two ligands. It is important to note that while ACh (**1**) and nicotine (**2**) complexes are close in their interaction energy values, the complex formed by epibatidine (**3**) represents the best of all the values, even the destabilization produced by the formation of the charge-transfer complex is minimized in this case.

A third level of analysis consists in examining the contribution of the individual ligand/fragment interactions to

Table 4
Pair-wise interaction energies (kcal/mol) corresponding to the SP approach at the B3LYP/6–31+g level of theory

Residue	ACh	Nicotine	Epibatidine
ASP83	−60.34	−73.59	−78.37
SER82	−3.81	−1.03	−1.99
ASP89	−74.25	−67.75	−78.76
TYR93	−2.23	−1.19	−0.10
TRP86	−2.56	−5.41	−9.76
TYR190	0.31	1.35	−1.45
TYR198	3.20	3.17	1.71
ARG209	−8.88	−9.95	−13.79
Total	−148.56	−154.40	−182.51

the total interaction energy. This information is collected in Table 4. The interactions within the (+) term, directly related with the positive end of the ligands are dominated by the ASP83 and ASP89 residues, with a lesser importance for the SER82 aminoacid. The relative weight of the contribution of ASP83 and ASP89 changes however a lot with the different ligands. In the case of ACh (**1**), ASP83 has a much smaller weight (−60.34 kcal/mol) than ASP89 (−74.25 kcal/mol), while the situation is inverted for nicotine (−73.59 kcal/mol versus −67.75 kcal/mol). Finally, epibatidine (**3**) presents the optimal value for the interaction with each of the two aminoacids (−78.37 and −78.76 kcal/mol, respectively). This optimal interaction with both aspartates is probably at the origin of the larger total interaction energy for this ligand. The effect of the third aminoacid within this term, SER82, is smaller, with a difference of <2 kcal/mol between the three ligands. Furthermore, it goes in the direction favoring ACh (**1**), opposite to the overall interaction.

Regarding π-cation interactions, it can be seen that the relative weight of both aminoacids, TYR93 and TRP86, changes completely in going from ACh (**1**) to epibatidine (**3**). TRP86 has always a stronger interaction, but the values are very near for ACh (−2.56 kcal/mol versus −2.23 kcal/mol), and very different in epibatidine (−9.76 kcal/mol versus −0.10 kcal/mol), with nicotine (**2**) lying in between (−5.41 versus −1.19 kcal/mol) when comparing with TYR93. TRP86 is therefore key in the fact that this term favors the epibatidine (3) complex. The charge transfer interactions (CTC) are more difficult to analyze, in line with the fact that they do not follow the overall trend. It is worth noticing however that, despite the identical nature of the two aminoacids involved, TYR190 and TYR198, the interaction is not symmetrical in any case. The (−) term, associated with the ligand negative end, is limited to one single aminoacid, ARG209. Therefore, it follows the trend of this term, discussed above, favoring much more epibatidine (**3**) than the other two ligands.

Taking all these data together, we can see that epibatidine-complex present the best structural arrangement for all the interactions, among the three studied ligands. The nicotine-complex, although displaying higher stabilization energy than the ACh-complex, occupies the second position in the ranking of stabilization energies. This relative order of total interaction energies is in good agreement with experimental data. So in a first approximation it can be stated that this model accounts for affinity trends and has the additional advantage that the computational time required for the calculations is affordable.

3.3. Effect of geometry relaxation

The analysis presented above has been based on interaction energies obtained from SP calculations on geometries taken from MD calculations. Although this is the only possible choice from the point of view of computational cost, one must be aware that these geometries do not correspond to the optimal arrangement for each single interaction. In what follows we will analyze how the geometry relaxation would affect the results. In order to carry out this evaluation, an additional set of calculations was carried out for one of the ligands, ACh (**1**), consisting of full geometry relaxation for each of the interacting pairs.

The geometry relaxation of each interaction was carried out at the same computational level as the energy evaluation, B3LYP/6–31+g. The results are collected in Table 5. There are three aspects from these calculations that deserve to be commented. The first of them is that, as expected, all the interaction energies yield better values, and those contributions that were repulsive in the above mentioned single-point approach (those in the CTC term), now become attractive. The second remarkable aspect is that the order of magnitude of interaction energies is practically unchanged when going from the single-point calculations to the much more expensive full relaxation. The interaction between the ligand and the two ASP residues are by far the most important, followed by the interaction with the ARG209 residue. The third result, which is not apparent in the Table, is that although the model is improved with the flexibility inherent in this approximation and is also promising in yielding the correct affinity trends as before, the lack of geometrical constraints leads to the overlap of the residues once the minimization has

Table 5
Interaction energies for the ACh-complex using two different approaches

Interaction	S.P.[a]	R.O.[b]
ACh–ASP83	−60.34	−78.02
ACh–SER82	−3.81	−4.46
ACh–ASP89	−74.25	−79.31
ACh–TYR93	−2.23	−4.54
ACh–TRP86	−2.56	−5.63
ACh–TYR190	0.31	−0.23
ACh–TYR198	3.20	−1.16
ACh–ARG209	−8.88	−19.30

Values are in kcal/mol.
[a] Single point approximation.
[b] Relaxed optimisation approximation.

been performed. For example, the position in which ASP83 is located after optimizing, is the actual position of SER82. Because of this, we consider that single-point calculations, despite all their limitations, are still a more reliable alternative than full relaxation for the problem under discussion.

Since these results showed the full relaxation scheme to be not efficient, a third approach was tried. This was labeled as partial relaxation, and consisted in relaxing part of the system while keeping frozen the position of the atoms attaching the aminoacids to the protein chain. The idea of this third approach was to allow the aminoacids to keep their relative orientations and avoid overlap of the residues, while improving their interaction with the ligands through the relaxation of some atoms, like for instance the polar hydrogens of serine and tyrosine. However, the trends in interactions energies, both values and behaviour, in the partial relaxation scheme were very close to those obtained in the SP approach described above. Because of this, and for the shake of simplicity, the results from the partial relaxation calculations will not be discussed.

4. Conclusions

From the earlier results and discussion, we can sum up the following conclusions:

1. Starting systems obtained from our previously published molecular mechanics/MD protocol seems to be an ideal guess to get a quantitative view of the main interactions occurring within nAChR and some of the more representative ligands.
2. The B3LYP hybrid density functional theory model, together with 6–31+g basis set is the best combination to get accurate results with reasonable time and computational resources.
3. The strategy adopted for the calculations, pairwise interactions, allows the discussion of the results at three different levels, as well as a way to estimate the relative weight of each kind of interactions within the binding site.
4. Among the three ligands studied, epibatidine (**3**) gives the stronger interaction, followed by nicotine (**2**) and ACh (**1**), showing the same trend as the biological affinities (pK_i) calculated experimentally.
5. Ionic interactions with the positive end of the ligand contribute the most at the total interaction energy, and mark the larger difference between the ligands. π-cation interactions follows in importance, and are also stabilizing. The charge transfer interactions have in contrast a destabilizing contribution to the total energy.
6. Geometry relaxed energies for the systems studied, although promising in yielding the correct affinity trends, would not produce an adequate image of the binding site, due to the overlap of different residues. Then, B3LYP/6–31+g SP calculations are the best approximation to be used in this case.

Similar calculations are being performed with other ligands to obtain a reliable data set to undertake QSAR analysis. These data would be relevant to discern which parts of the ligands are responsible for the main stabilization, and finally in the design of new compounds.

Acknowledgements

A.M. thanks the European Union (contract no. ERG FMGE CT95 0062), CESCA/CEPBA for a generous allotment of computer time during his stay at the UAB, and Consejo Social from the UA for financial support.

References

[1] D.J. Triggle, Pharmacological receptors: a century of discovery-and more, Pharm. Acta Helv. 74 (2000) 79–84.
[2] M.R. Bennett, The concept of transmitter receptors: 100 years on, Neuropharmacology 39 (2000) 523–546.
[3] C.M. Dobson, M. Karplus, The fundamentals of protein folding: bringing together theory and experiment, Curr. Opin. Struct. Biol. 9 (1999) 92–101.
[4] S. Sunyaev, W. Lathe III, P. Bork, Integration of genome data and protein structures: prediction of protein folds, protein interactions and molecular phenotypes of single nucleotide polymorphisms, Curr. Opin. Struct. Biol. 11 (2000) 125–130.
[5] N. Unwin, Nicotinic acetylcholine receptor at 9 Å resolution, J. Mol. Biol. 229 (1993) 1101–1124.
[6] N. Unwin, Acetylcholine receptor channel imaged in the open state, Nature 373 (1995) 37–43.
[7] J.-L. Galzi, J.-P. Changeux, Neurotransmiter-gated ion channels as unconventional allosteric proteins, Curr. Opin. Struct. Biol. 4 (1994) 554–565.
[8] A. Karlin, Structure of nicotinic acetylcholine receptors, Curr. Opin. Struct. Biol. 3 (1993) 299–309.
[9] J.-L. Galzi, J.-P. Changeux, Neural nicotinic receptors: molecular organization and regulations, Neuropharmacology 34 (1995) 563–582.
[10] H.R. Arias, Topology of ligand binding sites on the nicotinic acetylcholine receptor, Brain Res. Rev. 25 (1997) 133–191.
[11] F. Kotzyba-Hibert, T. Grutter, M. Goeldner, Molecular investigations on the nicotinic acetylcholine receptor, Mol. Neurobiol. 20 (1999) 45–59.
[12] P.-J. Corringer, N. Le Novère, J.-P. Changeux, Nicotinic receptors at the amino acid level, Annu. Rev. Pharmacol. Toxicol. 40 (2000) 431–458.
[13] M.W. Holladay, M.J. Dart, J.K. Lynch, Neural nicotinic acetylcholine receptors as targets for drug discovery, J. Med. Chem. 40 (1997) 4169–4194.
[14] J.D. Schmitt, Exploring the nature of molecular recognition in nicotinic acetylcholine receptors, Curr. Med. Chem. 7 (2000) 749–800.
[15] R.A. Glennon, M. Dukat, Nicotine receptor ligands, Med. Chem. Res. 26 (1996) 6465–6486.
[16] R.A. Glennon, M. Dukat, Nicotinic cholinergic receptor pharmacophores, in: S.P. Arneric, J.D. Brioni (Eds.), Neural Nicotinic Receptors: Pharmacology and Therapeutic Opportunities, Wiley, New York, 1999, pp. 271–284.
[17] R.A. Glennon, M. Dukat, Nicotine analogs: structure-affinity relationships for central nicotinic acetylcholinergic receptor binding, in: I. Yamamoto, J.E. Casida (Eds.), Nicotinoid Insecticides and the Nicotine Acetylcholine Receptor, Springer, Berlin, 1999, pp. 237–252.
[18] R.A. Glennon, M. Dukat, Central nicotinic receptor ligands and pharmacophores, Pharm. Acta Helv. 74 (2000) 103–114.

[19] J.E. Tonder, P.H. Olensen, Agonists at the α4β2 nicotinic acetylcholine receptors: structure-activity relationships and molecular modelling, Curr. Med. Chem. 8 (2001) 651–674.
[20] A.A. Bhat, E.W. Taylor, Structural evaluation of distant homology. A 3-D model of the ligand binding domain of the nicotinic acetylcholine receptor based on acetylcholinesterase: consistency with experimental data, J. Mol. Mod. 2 (1996) 46–50.
[21] M.O. Ortells, Prediction of the secondary structure of the nicoinic acetylcholine receptor nontransmembrane regions, Proteins Struct. Funct. Genet. 29 (1997) 391–398.
[22] N. Le Novère, P.-J. Corringer, J.-P. Changeux, Improved secondary structure predictions for a nicotinic receptor subunit: incorporation of solvent accessibility and experimental data into a two-dimensional representation, Biophys. J. 76 (1999) 2329–2345.
[23] E.E. Polymeropoulos, B. Kutscher, Epibatidine: a new lead for the design of non-opiate analgesics, in: F. Sanz, J. Giraldo, F. Manaut (Eds.), QSAR and Molecular Modelling: Concepts, Computational Tools and Biological Applications. Prous Science Publishers, Barcelona, 1995, pp. 608–610.
[24] M.H. Aprison, E. Gálvez-Ruano, K.B. Lipkowitz, The nicotinic cholinergic receptor: a theoretical model, J. Neurosci. Res. 46 (1996) 226–230.
[25] R.B. Westkaemper, Construction of three-helix models of the nicotinic receptor ligand binding site, Med. Chem. Res. 6 (1996) 511–525.
[26] E. Gálvez, I. Iriepa, A. Morreale, K.B. Lipkowitz, A computational model for the nicotinic acetylcholine binding site, J. Comput. Aided Mol. Design 13 (1999) 57–68.
[27] E.J. Barreiro, G. Barreiro, C.R.W. Guimaraes, R. Bicca de Alencastro, A new nicotine acetylcholine minireceptor model: a theoretical thermodynamics analysis of simultaneus cation-π and hydrogen bond interactions, J. Mol. Struct. (Theochem) 532 (2000) 11–22.
[28] A. Morreale, I. Iriepa, E. Gálvez, The 5-HT_3 and nACh ionotropic receptors: a perspective from the computational chemistry point of view, Curr. Med. Chem. 9 (2002) 99–125.
[29] K. Brejc, W.J. van Dijk, R.V. Klaassen, M. Schuurmans, J. van der Oost, A.B. Smit, T.K. Sixma, Crystal structure of an ACh-binding protein reveals the ligand-binding domain of nicotinic receptors, Nature 411 (2001) 269–276.
[30] Gaussian 98, Revision A.5, Gaussian Inc., Pittsburg, PA, 1998.
[31] J.C. Ma, D.A. Dougherty, The cation-π interaction, Chem. Rev. 97 (1997) 1303;
D.A. Dougherty, Cation-π interactions in chemistry and biology: a new view of benzene, Phe, Tyr, and Trp, Science 271 (1996) 163–168;
J.D. Schmitt, C.G.V. Sharples, W.S. Caldwell, Molecular recognition in nicotinic acetylcholine receptors: the importance of π-cation interactions, J. Med. Chem. 42 (1999) 3066–3074.